Particle Movement in Microelectrode Structures in AC Electric Fields, Under The Influence of Dielectrophoresis and Electrohydrodynamics

Nicolas G. Green

Royal Academy of Engineering Research Fellow
Department of Electronics and Electrical Engineering, University of Glasgow
Rankine Building, Oakfield Avenue, Glasgow G12 8LT, Scotland, UK
n.green@elec.gla.ac.uk

ABSTRACT

Dielectrophoresis is the movement of particles in suspension produced by interaction with non-uniform AC electric fields. Fields are typically generated by arrays of microelectrodes. Dielectrophoresis can be used for the non-contact manipulation, characterisation and separation of bioparticles in suspension.

However, the high strength electric fields (>10^5 V/m) required for the manipulation of sub-micrometre particles produce unavoidable fluid flow in many cases. There are two main types of fluid flow generated by non-uniform electric fields in microelectrode arrays: electrothermal fluid flow and AC electroosmosis. This paper presents simulations of the effect of these fluid flows and dielectrophoresis on the movement of particles. The effect of each mechanism in different frequency ranges is discussed.

Keywords: Dielectrophoresis, microelectrodes, particle manipulation, particle separation

1 INTRODUCTION

The use of AC electric fields for the manipulation, characterisation and separation of particles has become an area of considerable interest, both in basic research of the underlying physical mechanisms [1] and commercial application [2,3]. Dielectrophoresis (DEP) [4-6] has been applied to the manipulation and separation of a range of biological particles, such as cells and bacteria [4]. Recently, DEP has been applied to the manipulation and separation of a range of sub-micrometre and nanoscale particles [6-8].

Applications of dielectrophoresis require the fabrication of microelectrode arrays with typical dimensions of the order of micrometres to tens of micrometres. With electrodes of this size, even low applied potentials of the order of tens of volts produce high strength electric fields. An unavoidable consequence of these strong fields is that the suspending electrolyte is set in motion. Electric field-induced fluid flow can arise from several different physical mechanisms.

Electric field induced heating produces gradients in the electrical properties of the fluid, which result in a non-uniform induced charge distribution. The electric field then interacts with the gradients to produce a body force on the fluid and flow. This is electrothermal fluid flow [1], which occurs particularly at higher frequencies, around the charge relaxation frequency of the electrolyte. The second type of fluid flow arises from the interaction of the non-uniform electric field and the double layer it induces at the surface of the electrode. This type of fluid flow tends to zero at high and low frequency limits and is maximum at a frequencies of the order of kHz. This fluid flow is electro-osmotic in origin, is steady in non-uniform AC fields and is referred to as AC electroosmosis [9,10].

One type of electrode array has multiple applications for particle characterisation and separation. This is shown schematically in Figure 1 and consists of long interdigitated bar electrodes, energised alternately with an AC potential and ground. This paper presents Finite Element Method numerical simulations of each of the three effects: dielectrophoresis, electrothermal fluid flow and AC electro-osmosis. The motion of particles in different frequency regimes is then discussed.

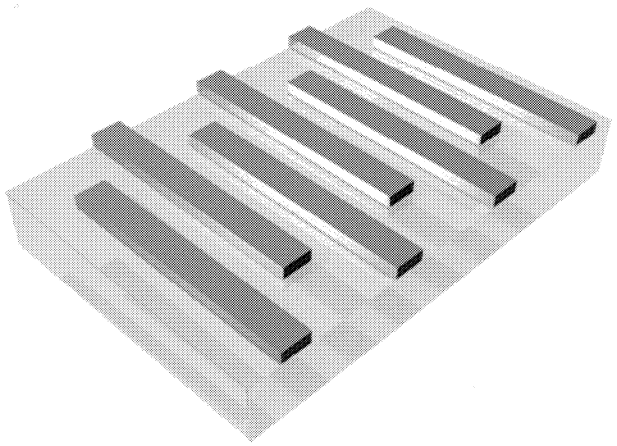

Figure 1. A schematic diagram of the interdigitated bar electrode array used in DEP applications. Typically, an AC potential and ground are applied to alternate electrodes and the particles are entrained over the array by a microchannel. In this paper an electrode array with electrodes of width 10 microns separated by gaps of 10 microns is simulated.

2 BACKGROUND AND THEORY

2.1 Dielectrophoresis

Dielectrophoresis is the movement of a particle produced by the interaction of a *non-uniform* electric field and the dipole it induces in the particle. For a spherical particle, the force is given by:

$$\langle \mathbf{F}_{DEP} \rangle = \pi \varepsilon_f a^3 \,\mathrm{Re}\left(\frac{\tilde{\varepsilon}_p - \tilde{\varepsilon}_m}{\tilde{\varepsilon}_p + 2\tilde{\varepsilon}_m} \right) \nabla |\mathbf{E}|^2 \qquad (1)$$

where a is the radius of the particle, $\mathbf{E}$ is the electric field, e_f is the permittivity of the suspending fluid and Re(...) indicates the real part of the term in brackets, which is referred to as the Clausius-Mossotti (CM) factor. The CM factor is derived from the polarisation of the particle/fluid interface and is a function of the complex permittivities of the particle, $\tilde{\varepsilon}_p$, and the fluid, $\tilde{\varepsilon}_f$. A general complex permittivity is given by $\tilde{\varepsilon} = \varepsilon - i\sigma/\omega$, where ε is the permittivity, σ is the conductivity and ω is the angular frequency of the applied harmonic electric field.

The dielectrophoretic force is determined numerically by solving Laplace's equation for the electrical potential ϕ over the problem space and calculating the electric field term in equation (1) as $\nabla |\mathbf{E}|^2 = \nabla |\nabla \phi|^2$. The application of this method for DEP is described in detail elsewhere [11].

2.2 Electrothermal fluid flow

Numerical simulation of the fluid flow is performed in stages, as described previously for a different electrode geometry [12]. First the electrical potential is solved as in the previous section. Second, the thermal field in the device is simulated using the heat diffusion equation:

$$k\nabla^2 T + \left\langle \sigma |\mathbf{E}|^2 \right\rangle = 0 \qquad (2)$$

where T is the temperature, k the thermal conductivity and the source term is the time averaged Joule heating. Once the thermal field has been solved, the body force everywhere on the fluid can be calculated from

$$\langle \mathbf{f}_e \rangle = \frac{\varepsilon_f}{2} \mathrm{Re}\left(\frac{\alpha - \beta}{1 + i\omega\varepsilon_f/\sigma_f} (\nabla T \cdot \nabla \phi) \nabla \phi - \frac{\alpha}{2} |\nabla \phi|^2 \nabla T \right) \qquad (3)$$

where $\alpha = (1/\varepsilon)(\partial\varepsilon/\partial T)$ and $\beta = (1/\sigma)(\partial\sigma/\partial T)$ are approximately equal to $-0.4\%\mathrm{K}^{-1}$ and $2\%\mathrm{K}^{-1}$ for an aqueous electrolyte. The fluid velocity $\mathbf{u}$ is then calculated from the Navier-Stoke's equation reduced to:

$$-\nabla p + \eta \nabla^2 \mathbf{u} + \langle \mathbf{f}_e \rangle = 0 \qquad (4)$$

where p is the pressure and η is the viscosity of the fluid.

2.3 AC Electroosmosis

The physical mechanism responsible for AC Electro-osmosis is shown schematically in Figure 2. The method for numerical simulation has been described previously for a different electrode geometry [10]. In summary, the slip velocity at the surface of the electrode is calculated from the electrical stress on the double layer. The stress is determined by solving Laplace's equation for the electrical potential ϕ with the boundary condition

$$\phi_B = V + \sigma Z_{DL} \frac{\partial \phi_B}{\partial n} \qquad (5)$$

where V is the amplitude of the applied voltage, n is the normal direction and Z_{DL} is the measured frequency dependent impedance of the electrical double layer on the electrode. The potential is then solved as a function of frequency and the frequency dependent slip velocity at the electrode surface calculated from:

$$\langle u_{slip} \rangle = -\frac{\varepsilon_f}{4\eta} \frac{\partial}{\partial t} |\phi_B - V|^2 \qquad (6)$$

where t is the tangential direction. The bulk fluid motion is then solved from equation (5), with zero body force and equation (6) as the boundary condition on the electrode.

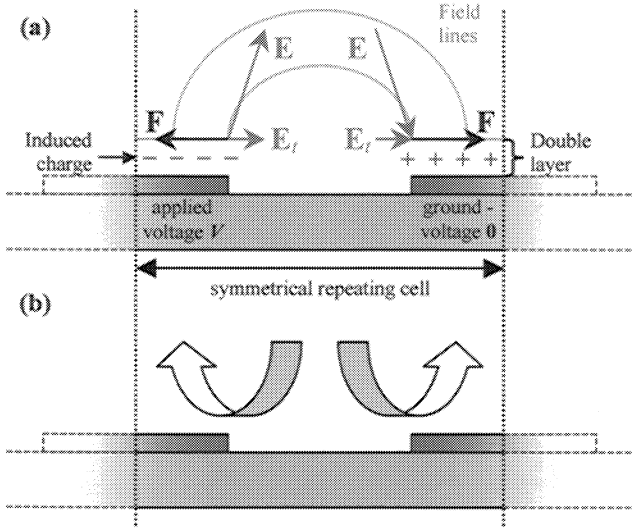

Figure 2. A schematic diagram illustrating the physical mechanism of AC electroosmosis (a) and the resulting bulk fluid motion (b). The tangential component of the electric field exerts a non-zero time averaged force **F** on the induced charge at the electrode surface producing flow.

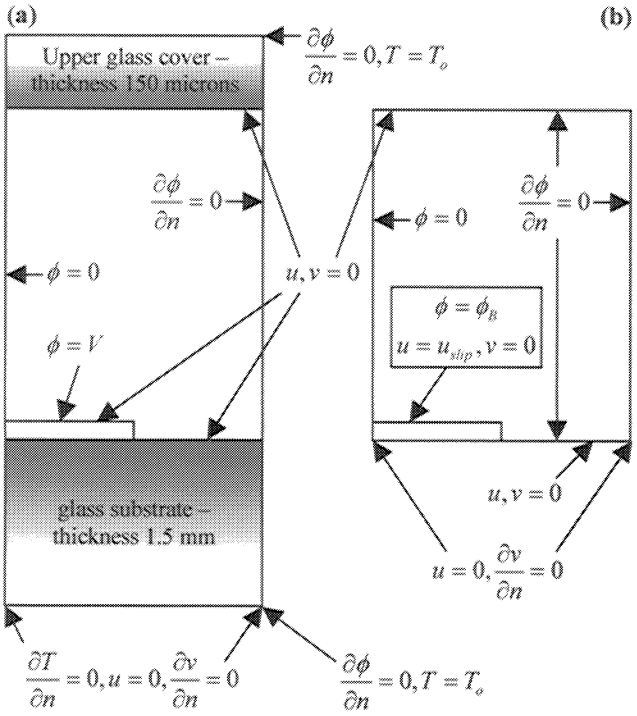

Figure 3. A schematic diagram of the problem spaces for (a) the dielectrophoretic and electrothermal fluid flow problems and (b) the AC electroosmosis problem. In both cases, u is the horizontal and v is the vertical component of the fluid velocity. The problem space consists of one half of an electrode and half of the adjacent gap and appropriate symmetry boundary conditions to create the image of an infinite array.

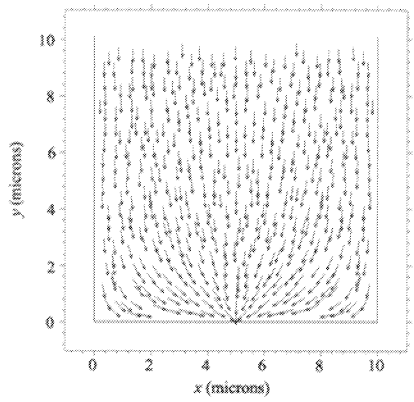

Figure 4. Numerically calculated direction (a) and magnitude (b) of $\nabla|\nabla\phi|^2$ for the 10micron electrode array and an applied voltage of 2V.

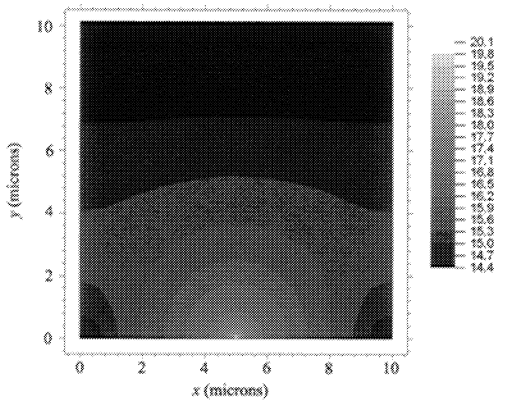

3 NUMERICAL SIMULATION

Numerical simulations were performed using a generic Partial Differential equation solver FlexPDE [13]. The solver uses the Finite Element Method, with equations, problem spaces and boundary conditions defined by descriptor files. The problem space is divided into triangular elements and the solution of each variable within the element approximated by a third order polynomial. The problem space for the DEP and electrothermal problems is shown in Figure 3a and for the AC electroosmosis problem in Figure 3b.

3.1 Dielectrophoresis

The solution for the term $\nabla|\nabla\phi|^2$, which can be inserted into equation (1) to calculate the dielectrophoretic force for a specific particle, is shown in Figure 4 for the interdigitated electrode array. The vector points towards the strong electric field region close to the electrode edge, with a rapidly increasing magnitude with decreasing distance. In this electrode array, a 100nm particle would experience a maximum DEP velocity of ~10microns/s at the edge.

3.2 Electrothermal fluid flow

The numerically calculated fluid flow driven by the electrothermal mechanism is shown in Figure 5. At low electrolyte conductivities, e.g. 2mS/m, the fluid velocity can be of the order of 10microns/s, with a single roll over the electrode edge. At high frequencies, above the charge relaxation frequency ~σ/ε (~1MHz), there is a complicated pattern of fluid flow due to the balance of the two terms in the force expression (equation (3)) but the fluid velocity is much lower in magnitude.

3.3 AC electroosmosis

The numerically calculated bulk AC electroosmotic fluid flow is shown in Figure 6 for an applied field frequency of 10kHz, close to the maximum in fluid velocity. There is a single roll over the electrode edge with very high velocities (>1mm/s) at the electrode surface. This flow can be significantly stronger than dielectrophoresis at low frequencies, preventing the collection of particles at the electrode but rapidly diminishes with increasing frequency.

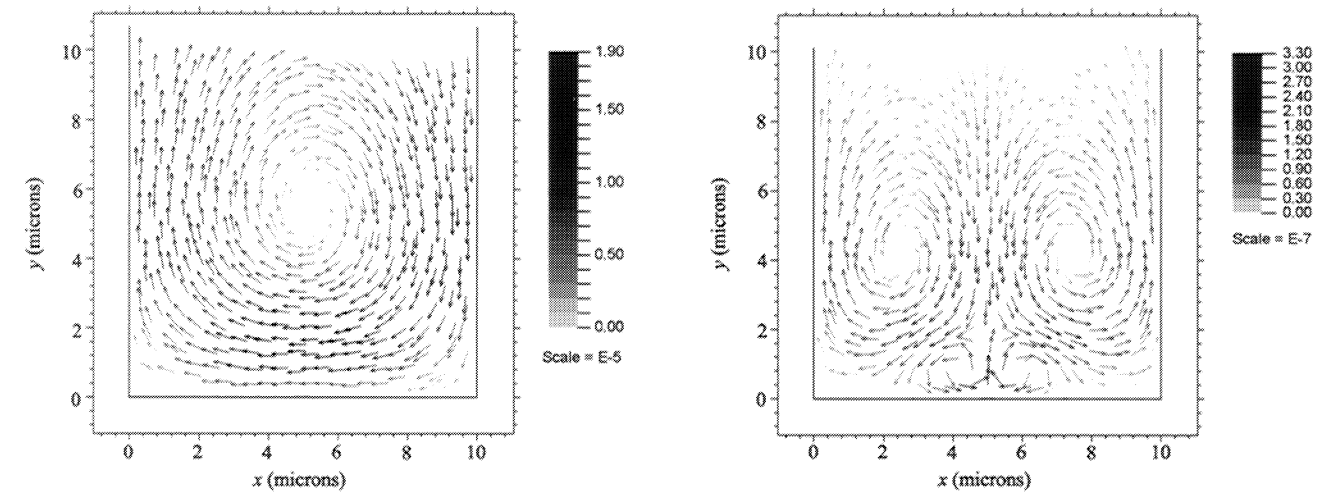

(a) (b)

Figure 5. Numerically calculated electrothermal fluid velocity for an applied voltage of 10 volts in a electrolyte conductivity of 2mS/m at (a) low frequencies and (b) high frequencies. There is a substantial change in flow pattern and magnitude .

CONCLUSIONS

The fluid flow in a widely used DEP electrode array due to two mechanisms: electrothermal and AC electroosmosis has been simulated. The fluid flow is strong at particular frequencies and can disrupt dielectrophoretic motion but, in general, becomes negligible with increasing frequency. An accurate determination of the movement of particles in this type of electrode based microsystem is essential to its operation. These results will be of interest to researchers using dielectrophoresis based analysis and separation systems.

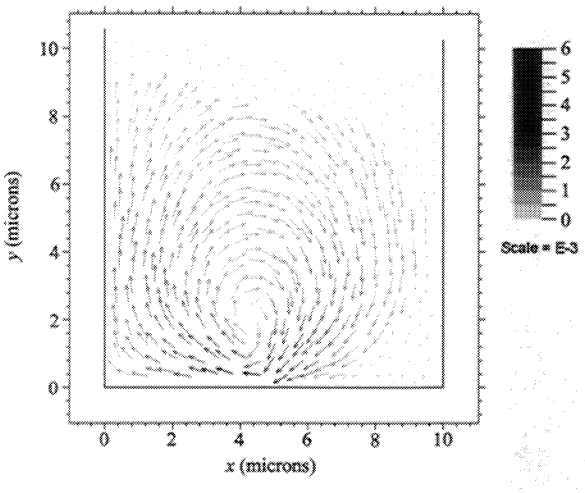

Figure 6. Numerically calculated AC electroosmotic fluid flow for the interdigitated electrode array and an applied voltage of 2 volts at 10kHz. The fluid moves down onto the electrode surface, with the highest velocities found close to the edge.

ACKNOWLEDGEMENTS

The author would like to thank the Royal Academy of Engineering, UK for the award of a Fellowship and Prof. Hywel Morgan (University of Glasgow) and Dr Antonio Ramos (University of Sevilla) for valuable discussions.

REFERENCES

[1] A.Ramos, H.Morgan, N.G.Green and A.Castellanos J. Phys. D: Appl. Phys. **31** p2338-2353 (1998).
[2] http://www.nanogen.com/invest_news/patents.asp.
[3] http://www.cytopulse.com/4000101.html.
[4] R.Pethig Crit. Revs. Biotechnol. 60 331-348 (1996).
[5] T.B.Jones "Electromechanics of Particles" Cambridge Univ. Press, Cambridge (1995).
[6] H.Morgan and N.G.Green "AC Electrokinetics: Colloids and Nanoparticles", Research Studies Press, Baldock, Herts., UK (2003).
[7] M.Washizu, S.Suzuki, O.Kurosawa, T.Nishizaka and T.Shinohara IEEE Trans. Ind. Appls 30 835-843 (1994).
[8] H.Morgan, M.P.Hughes and N.G.Green Biophys. J. 77 516-525 (1999).
[9] N.G.Green, A.Ramos, A.González, H.Morgan and A.Castellanos Phys. Rev. E 61 4011-4018 (2000).
[10] N.G.Green, A.Ramos, A.González, H.Morgan and A.Castellanos Phys. Rev. E 66 art.no.0263XX (2002).
[11] N.G.Green, A.Ramos and H.Morgan J. Electrostatics 56 235-254 (2002).
[12] N.G.Green, A.Ramos, A.González, H.Morgan and A.Castellanos J. Electrostatics 53 71-87 (2001).
[13] www.pdesolutions.com